EFFECT OF REYNOLDS NUMBER ON THE FLOW ABOUT A FINITE CONE OF 70 DEGREES

Thesis by

Lt. Cmdr. William R. Bottenberg, USN

In Partial Fulfillment of the Requirements

for the Degree of Aeronautical Engineer

California Institute of Technology

Pasadena, California

1949

ACKNOWLEDGMENTS

The investigation was conducted under Mr. Allen E. Puckett for whose help and advice deep appreciation is hereby expressed. The work was done jointly with Cdr. R. A. Bevernick, USN. Information on maximum permissible humidity limits was given by Mr. Richard Head.

ABSTRACT

An investigation was made to determine the effect of Reynolds number on the flow about a cone of 70 degrees apex angle with free stream Mach numbers close to the Mach number for shock attachment.

Conditions existing on the forward half of a one-half inch diameter cone were investigated at two Mach numbers, one giving a slightly detached shock and one giving a slightly attached shock, at Reynolds numbers from 150,000 to 1,300,000 based on model diameter.

Close to the apex the static pressure on the surface of the cone divided by the stagnation pressure before the shock was found to be dependent upon the Reynolds number at the lowest Reynolds number when the shock was detached but not when the shock was attached. In both cases at a distance half way back on the cone there was a continuous increase in this ratio with increasing Reynolds number. All of these Reynolds number effects were small in magnitude.

The investigation was conducted in the GALCIT 2.5" Supersonic Wind Tunnel.

TABLE OF CONTENTS

LIST OF FIGURES

I. INTRODUCTION

Investigations conducted by Marschner and Altseimer, Ref. 1, indicated the possibility that the detached shock wave on a large angle cone in a flow with free stream Mach number close to shock attachment might not be a normal shock at the nose of the cone as given by theory. If such a phenomenon existed, the central streamline would have to be turned through some small angle which would result in the formation of a small needle-like region of dead air between the shock wave and the apex of the cone. This dead air region, if it existed, would be a viscous phenomenon and should thus be effected by Reynolds number.

The purpose of the present investigation was to determine the effect of Reynolds number on the flow field about a finite cone of 70 degrees with free stream Mach numbers close to the Mach number for shock attachment.

The criterion used for determining whether or not Reynolds number effects existed was the static pressure on the surface of the cone divided by the stagnation pressure before the shock wave. The static pressure was measured on the forward half of the cone. The two Mach numbers investigated were $M = 1.64$, which was slightly less than the Mach number for shock detachment, and $M = 1.72$, which was slightly greater than the shock detachment Mach number, $M = 1.683$. The overall Reynolds number range was from about $R_N = 150{,}000$ to approximately $R_N = 1{,}300{,}000$ based on model diameter.

II. EQUIPMENT

The wind tunnel used for this investigation was the GALCIT 2.5" Supersonic Wind Tunnel, which is described in Ref. 2. It is a closed throat, single return type with a test section 2.5 inches square, and fixed nozzle blocks were used for both Mach numbers. The nozzle blocks for M = 1.64 were constructed of steel and formed a test section of 2.5" x 2.5". The centerline survey showing the Mach number distribution for this nozzle along a line through the axis of the model, is shown in Fig. 1. The nozzle blocks for M = 1.72 were constructed of polished maple and formed a test section of 2.5" horizontally by 2.0" vertically. These wooden blocks were originally designed to place the test section considerably forward of the model support used in this investigation. They were modified by moving the blocks aft so that the test section was in proper position with respect to the sting and using maple filler blocks before the throat. The Mach number distribution along a line through the model axis for the M = 1.72 nozzle is shown in Fig. 2.

The centerline Mach number surveys were made by attaching one end of a long hypodermic needle to the sting by means of a clamp. The other end was supported in the subsonic portion of the nozzle. There were two orifices on the sides of the needle, spaced 180 degrees apart, to measure the static pressure. The pressure was led from the needle at the forward end in the subsonic portion of the nozzle. By moving the needle through the clamp the orifice could be positioned axially. A series of static pressure measurements were made in the vicinity of

the model location. The difference between centerline static pressure and wall static pressure was measured on an acetylene tetrabromide manometer. The difference between wall static pressure and atmospheric pressure was measured on a mercury manometer.

The models tested were constructed of brass and are shown in Fig. 3. The choice of one-half inch model diameter was made on the basis of blocking data for the wind tunnel given in Ref. 1, Fig. 64. In order to simplify the construction of the models, a separate model was made for each desired static pressure orifice location. Since it was desired to investigate only the forward portion of the nose, four static pressure orifice locations forward of the mid-point of the cone were selected. An attempt was made to locate one orifice as close to the apex as possible. For this reason, the orifice on this model is only .006 inches in diameter, whereas the other orifices are .013 inches in diameter. An apex angle of 70 degrees was selected because theoretical data for a 70 degree cone are given in the Kopal Report, Ref. 3.

Pictures of the shock phemonena were taken by means of a Schlieren apparatus, described in Ref. 2. An exposure time of 1/500,000 sec. was given by the spark system.

III. PROCEDURE

After conducting the centerline Mach number survey on a nozzle one of the four models was attached to the sting and set at zero angle of attack. The static pressure, P_x', and settling tank pressure, P_o, measured on mercury manometers, were then obtained for a series of Reynolds numbers. Also the pressure at a series of static pressure orifices located axially along the upper test section wall was read on mercury manometers for comparison of the Mach numbers during different runs. Dew point temperature and stagnation temperature before the shock wave were also recorded. This procedure was followed with each nozzle and with all four models.

Since the mechanism used in adjusting angle of attack did not indicate an absolute setting, the model was set on zero angle of attack by reading static pressure for several angles of attack relative to an arbitrary setting with the orifice up and repeating with the orifice down. Zero angle of attack was taken as the position which gave the same pressure with the orifice up or down. This procedure had an additional benefit in tending to minimize the effect of any stream angle in the flow. Sample plots of P_x' vs. α are shown in Fig. 4.

Reynolds number was varied by varying the density of air in the tunnel. High Reynolds number was obtained by manipulating valves so that the pressure was built up in the settling tank. The air taken in made only one pass through the de-humidifier. After building up the desired pressure the de-humidifier was cut out of the system,

since it could not withstand pressure or suction, and a valve was opened to allow the air to circulate through the tunnel. Low Reynolds numbers were obtained in a similar manner except that air was taken out of the settling tank to reduce the density. In this case also the de-humidifier had to be cut out of the system before starting flow through the tunnel.

In order to obtain consistent data it was necessary to maintain the humidity of the air in the tunnel at as low a level as possible. When the tunnel was running at near atmospheric pressure the de-humidifier could be left in the system and a low value of relative humidity obtained since the air was being dried continuously. When operating at high pressures, a large portion of the air in the tunnel had made just one pass through the de-humidifier and the relative humidity tended to be appreciably higher. With low tunnel pressure any leaks in the portions of the tunnel where sub-atmospheric pressures existed, allowed wet air to leak into the system. For these reasons, the tunnel was run at atmospheric pressure with the de-humidifier in the system for a long enough period to reduce the relative humidity to the lowest attainable value before starting a high or low pressure run. Also, readings were taken as soon as possible after the start of a high or low pressure run. Using these methods it was possible to hold the relative humidity between 1.0 to 4.5% at atmospheric tunnel pressures, between 3.0 to 5.5% at low tunnel pressures, and between 8 to 13.5% at high tunnel pressures. On the basis of research being conducted at GALCIT these relative humidities were low enough to assure that no condensation shocks occurred.

All runs were viewed by means of the Schlieren apparatus and pictures of representative runs were taken.

IV. REDUCTION AND PRESENTATION OF DATA

The static pressure, P_x', at each orifice location, was reduced to a dimensionless ratio by dividing it by P_o, the stagnation pressure in the settling tank (which is also the stagnation pressure before the shock), to give P_x'/P_o. The location of each orifice was reduced to a dimensionless ratio by dividing x', the distance between the apex of the cone and the center of the orifice, by s, the slant length of the cone from the apex to the shoulder, to give x'/s. Reynolds number was computed from the stagnation temperature, stagnation pressure, and the Mach number, using Fig. 10 of Ref. 4. Relative humidity was computed from the dew point temperature and stagnation temperature.

Data showing P_x'/P_o vs. Reynolds number for various values of x'/s are presented in Figs. 5 to 9. Cross-plots of this data showing P_x'/P_o vs. x'/s for various values of Reynolds number are presented in Figs. 10 and 11.

Six contact photographs taken of high, intermediate and low Reynolds number at each Mach number are presented in Figs. 12 to 17. Enlargements of the intermediate Reynolds number at each Mach number are shown in Figs. 18 and 19. Fig. 20 shows the traces of the shock waves made by projecting the negative on graph paper and sketching in the lines.

V. DISCUSSION

It is of value to consider those features of the flow over the finite cone which can be treated by theory. Taylor and Maccoll, Ref. 5, developed methods of calculating the flow about cones when the flow field is conical. Conical flow about a finite cone is obtained only when the shock wave is attached and when the flow behind the shock wave is supersonic. The Kopal report, Ref. 3, gives the solution for a 70 degree cone and indicates that the shock wave is detached for Mach numbers less than 1.683 and that the flow close to the cone behind the shock wave is subsonic for Mach numbers less than 1.91. Thus, on the basis of theory, it can be predicted for a finite 70 degree cone that:

1. At M = 1.72

   a. The shock wave is attached.

   b. The flow behind the shock wave along the cone is subsonic making it possible for the effect of the disturbance at the shoulder to be propagated upstream.

   c. The flow field behind the shock wave is non-conical resulting in non-uniform pressure between the apex and shoulder.

   d. The pressure should decrease from the apex to the shoulder because of acceleration of the subsonic flow.

   e. The pressure should approach the conical flow value $P_x'/P_o = .591$ at the apex.

   f. The shock wave angle should approach the conical flow value of $\Theta_w = 64.2$ degrees at the apex.

2. At M = 1.64

a. The shock wave is detached.

b. The shock wave is a normal shock at the apex.

c. The flow behind the shock wave along the cone is subsonic making it possible for the effect of the disturbance at the shoulder to be propagated upstream.

d. The flow field behind the shock wave is non-conical resulting in non-uniform pressure between the apex and shoulder.

e. The pressure should decrease from the apex to the shoulder because of acceleration of the subsonic flow.

f. The pressure at the apex should approach the stagnation pressure downstream of a normal shock of $P_x'/P_o = .879$.

Consider first the condition with the shock wave slightly detached, M = 1.64. From Fig. 10 it is seen that close to the apex the static pressure begins to rise sharply and apparently approaches the theoretical value at the apex. The theoretical P_x'/P_o is indicated by the small arrow at $P_x'/P_o = 0.879$, which is based on the stagnation pressure ratio through a normal shock at Mach number 1.64. The data obtained by Marschner and Altseimer, Ref. 1, had a minimum x'/s of 0.2, and there was some question that the static pressure, forward of this point, would rise rapidly enough to reach the theoretical P_x'/P_o for a normal shock at the apex. If it did not, it would have been an indication that the theoretical detached normal shock at the apex was actually an oblique shock wave.

Fig. 10 appears to indicate rather conclusively that the theoretical P_x'/P_o is reached at the cone apex and therefore, the shock wave is normal at the apex. This is further indicated by the Schlieren pictures Fig. 12 to 14, and Fig. 18.

The data plotted in Fig. 5 indicate that for all values of x'/s tested, P_x'/P_o tends to drop at the lowest Reynolds number. This probably results from increased boundary layer thickness along the cone surface at the low Reynolds number. At $x'/s = 0.5$ the plot drops continuously down to the left. Apparently the Reynolds number has an increasing effect as the x'/s increases. This could possibly be explained by the influence of Reynolds number on the disturbance created at the shoulder being propagated upstream into the subsonic flow along the cone.

With the shock wave attached at $M = 1.72$ the data of Figs. 6 to 8 indicate no Reynolds number effects on the static pressure for x'/s up to 0.2. At $x'/s = 0.5$, Fig. 9, the line again slopes down to the left indicating a Reynolds number effect. This appears to confirm the similar result obtained at $M = 1.64$. In Fig. 11, P_x'/P_o is plotted against x'/s for three Reynolds numbers. Theoretical results, verified by the data of Marschner and Altseimer, Ref. 1, show that, when the shock wave is attached but the flow over the cone is subsonic, the static pressure on the cone drops smoothly as x'/s increases. This is because the flow is accelerating from the apex of the shoulder. The arrow in Fig. 11 indicates the theoretical $P_x'/P_o = .591$ at the apex, obtained from data in Ref. 3. It is seen that the data for

x'/s = .0436 lies considerably above this value. It is believed that this was caused by slight damage sustained by this model. The damage was a small oblique area of bluntness at the apex, opposite the static pressure orifice. It if felt that the damage caused a rise in static pressure but that it did not invalidate the results of Fig. 6; namely that there was no effect with Reynolds number. The slope downward from left to right, in Fig. 11, is believed to be less than it should be. That is, the $P_{x'}/P_o$ data for x'/s = 0.2 and 0.5 appear to be a little too high by comparison with Ref. 1. This may be a result of the rather poor Mach number distribution obtained with the nozzle used for M = 1.72. The plot was made with dashed lines to indicate the magnitude of the Reynolds number effect, but as previously stated, it is felt that the lines should drop off more rapidly to the right. The shock wave angle measured on Fig. 20 was Θ_w = 64 degrees which compares favorably, within the limits of accuracy of measurement, with the theoretical value of Θ_w = 64.2 degrees.

It should be pointed out that an expanded scale has been used for $P_{x'}/P_o$; thus the Reynolds number effects are actually small.

VI. CONCLUSIONS

The results of this investigation indicate that there are Reynolds number effects associated with the flow about a finite cone in a supersonic stream when the free stream Mach number is low enough to give subsonic velocities on the surface of the cone. For the 70 degree cone investigated these effects are as follows:

1. With a slightly detached shock wave at $M = 1.64$, P_x'/P_o increases with Reynolds number at points on the forward two-tenths of the cone until Reynolds number equals 430,000, and thereafter remains constant.
2. With a slightly detached shock wave at $M = 1.64$ or a slightly attached shock wave at $M = 1.72$, P_x'/P_o increases continuously with Reynolds number at points located farther back on the cone than $x'/s = .2$ in the range of Reynolds number and x'/s investigated.

It is also concluded that with a detached shock wave in a stream with the Mach number close to that for shock attachment, the shock wave is normal at the apex of the cone, and the static pressure at the apex is as given by theory.

REFERENCES

1. Marschner, B. W., "An Investigation of Detached Shock Waves", Thesis, California Institute of Technology, 1948.

2. Puckett, A. E., and Schamberg, R., "Final Report - Galcit Supersonic Wind Tunnel Tests", Library of Aeronautics Department, California Institute of Technology, June, 1946.

3. Kopal, Z., "Supersonic Flow Around Cones", Massachusetts Institute of Technology, Center of Analysis, Report No. 1, 1947.

4. NACA Technical Note No. 1428, "Notes and Tables for Use in the Analysis of Supersonic Flow, December, 1947.

5. Taylor, G. I., and Maccoll, J. W., "The Air Pressure on a Cone Moving at High Speeds", Proc. Royal Soc. of London, 1933, Vol. 139.

FIG. 1

CENTERLINE SURVEY
Mach = 1.64

SHOCK DETACHED

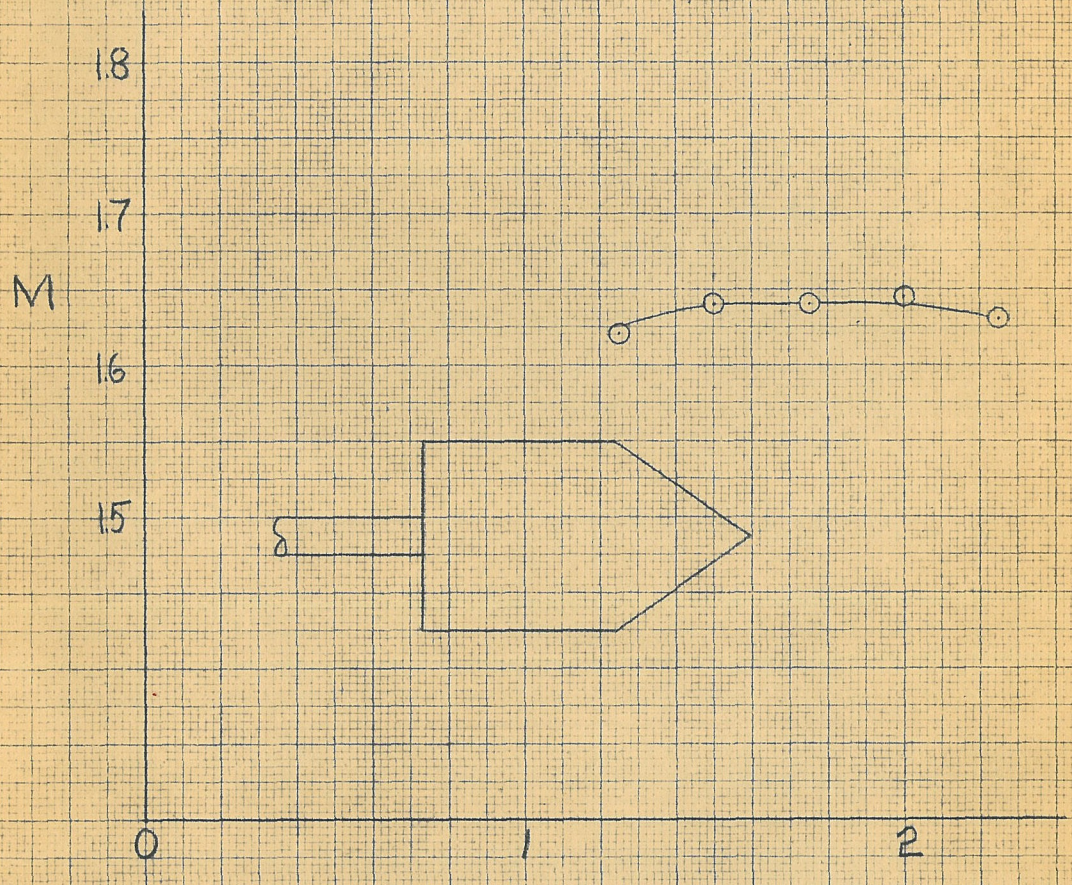

FIG. 2

CENTERLINE SURVEY
Mach = 1.72

SHOCK ATTACHED

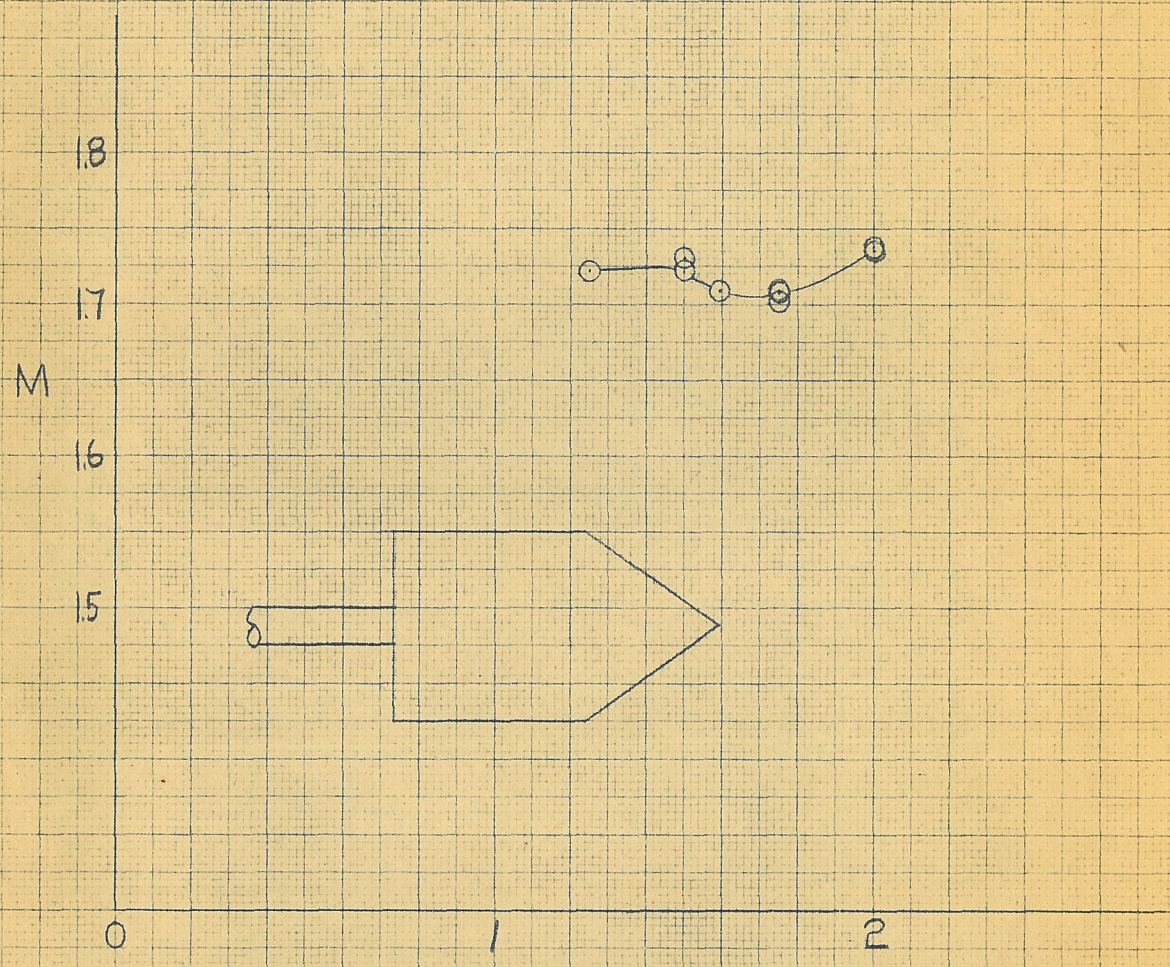

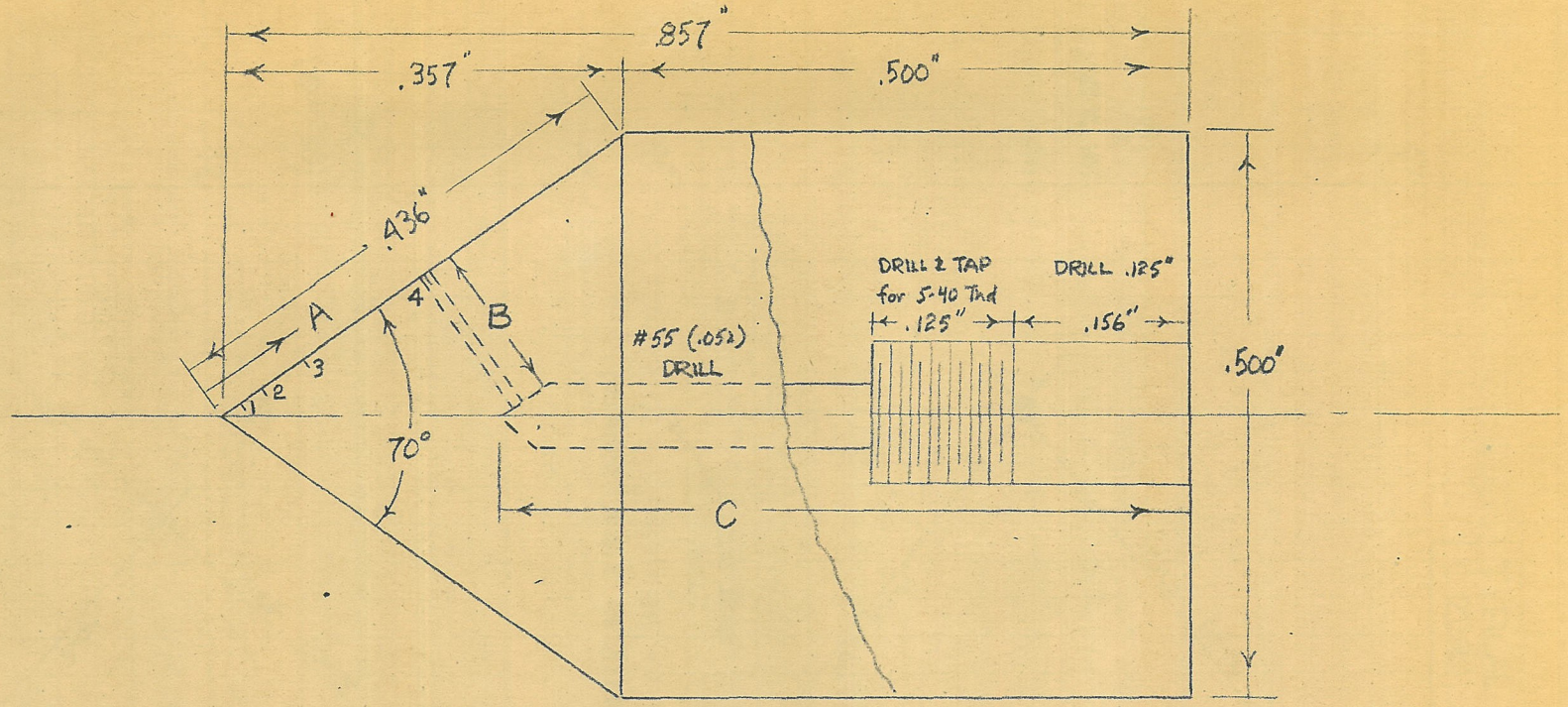

FIG. 3

CONE MODELS

Cone No.	A	B	C	ORIFICE DIAM.
1	.019	.014	.840	.006" PIVOT DRILL
2	.044	.031	.803	#80 DRILL (.013")
3	.088	.061	.751	"
4	.218	.153	.591	"

FIG. 4

TYPICAL DETERMINATION OF ZERO ANGLE OF ATTACK

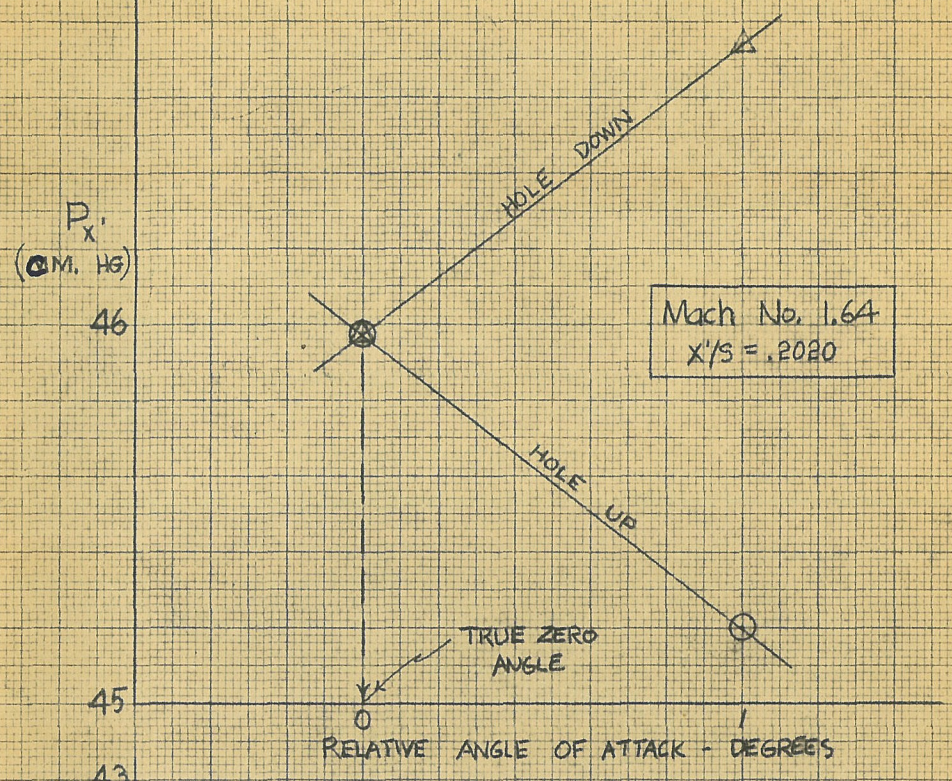

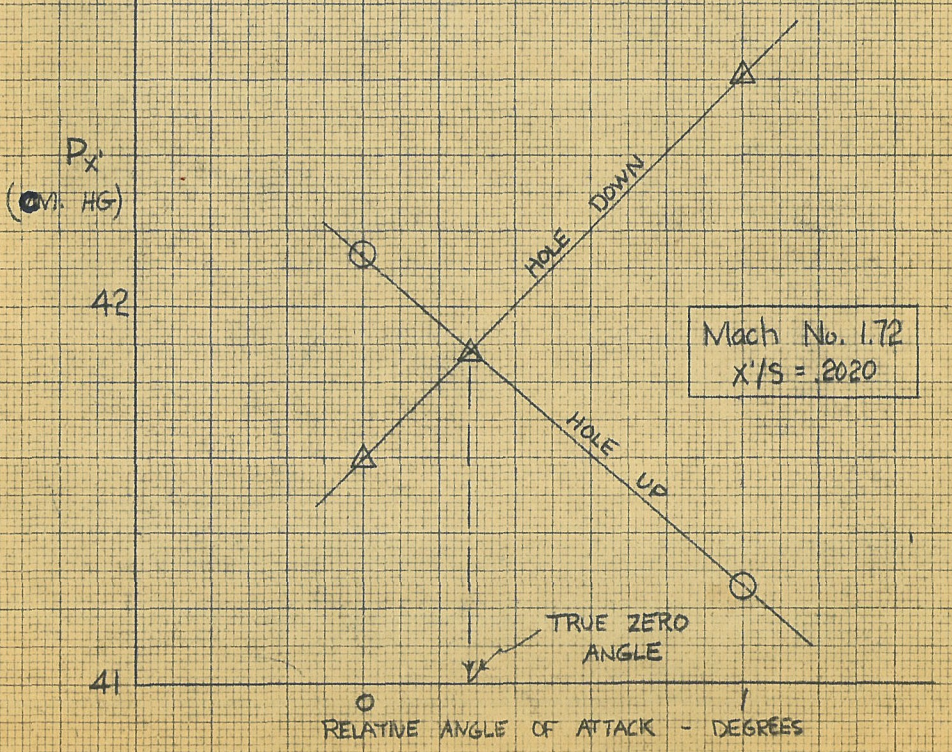

Fig. 5

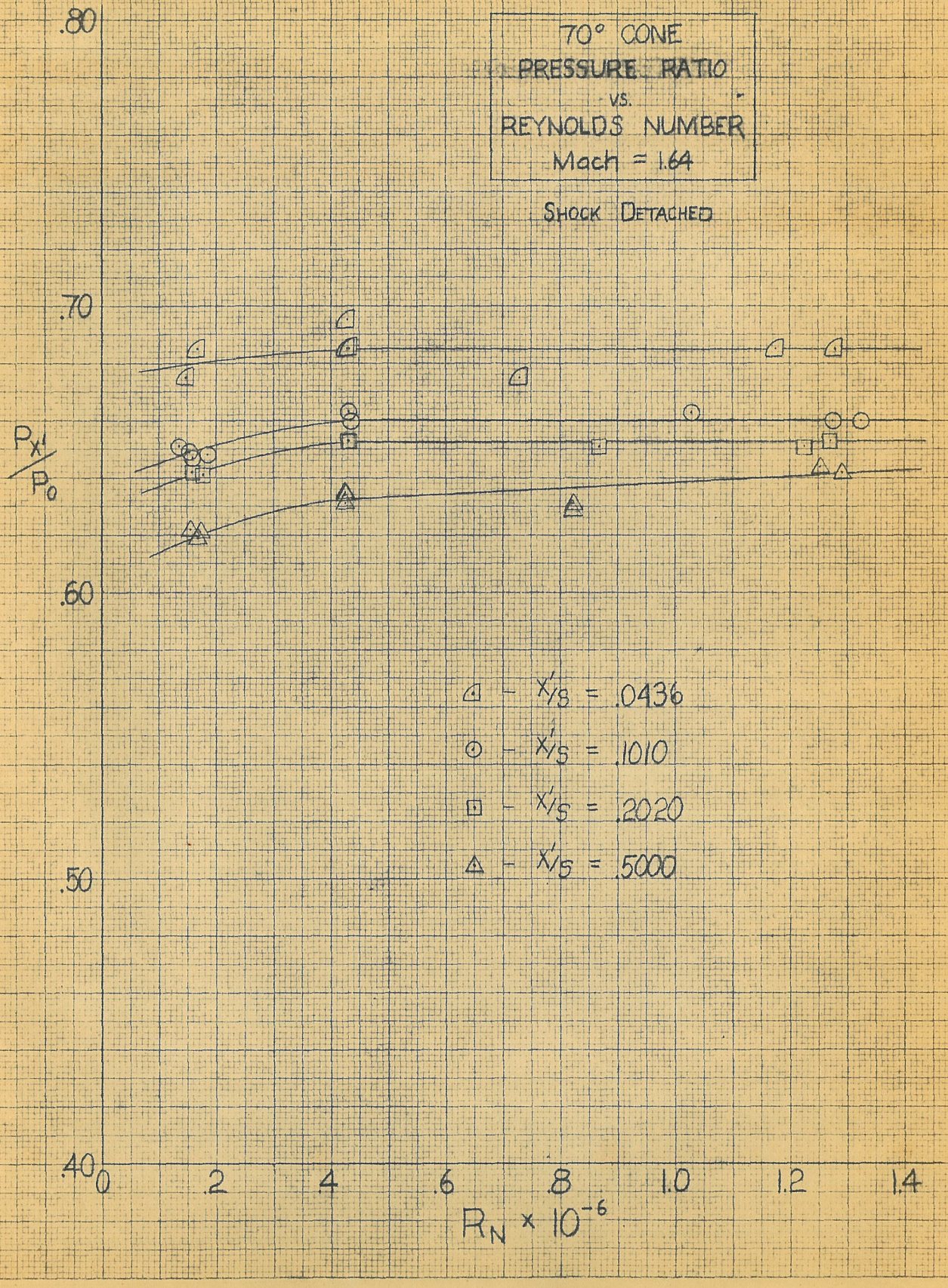
70° CONE
PRESSURE RATIO
VS.
REYNOLDS NUMBER
Mach = 1.64
SHOCK DETACHED
.80
.70
.60
.50
.40
$P_{x'}/P_0$
△ - X'/S = .0436
⊙ - X'/S = .1010
□ - X'/S = .2020
△ - X'/S = .5000
0
.2
.4
.6
.8
1.0
1.2
1.4
$R_N \times 10^{-6}$

FIG. 6

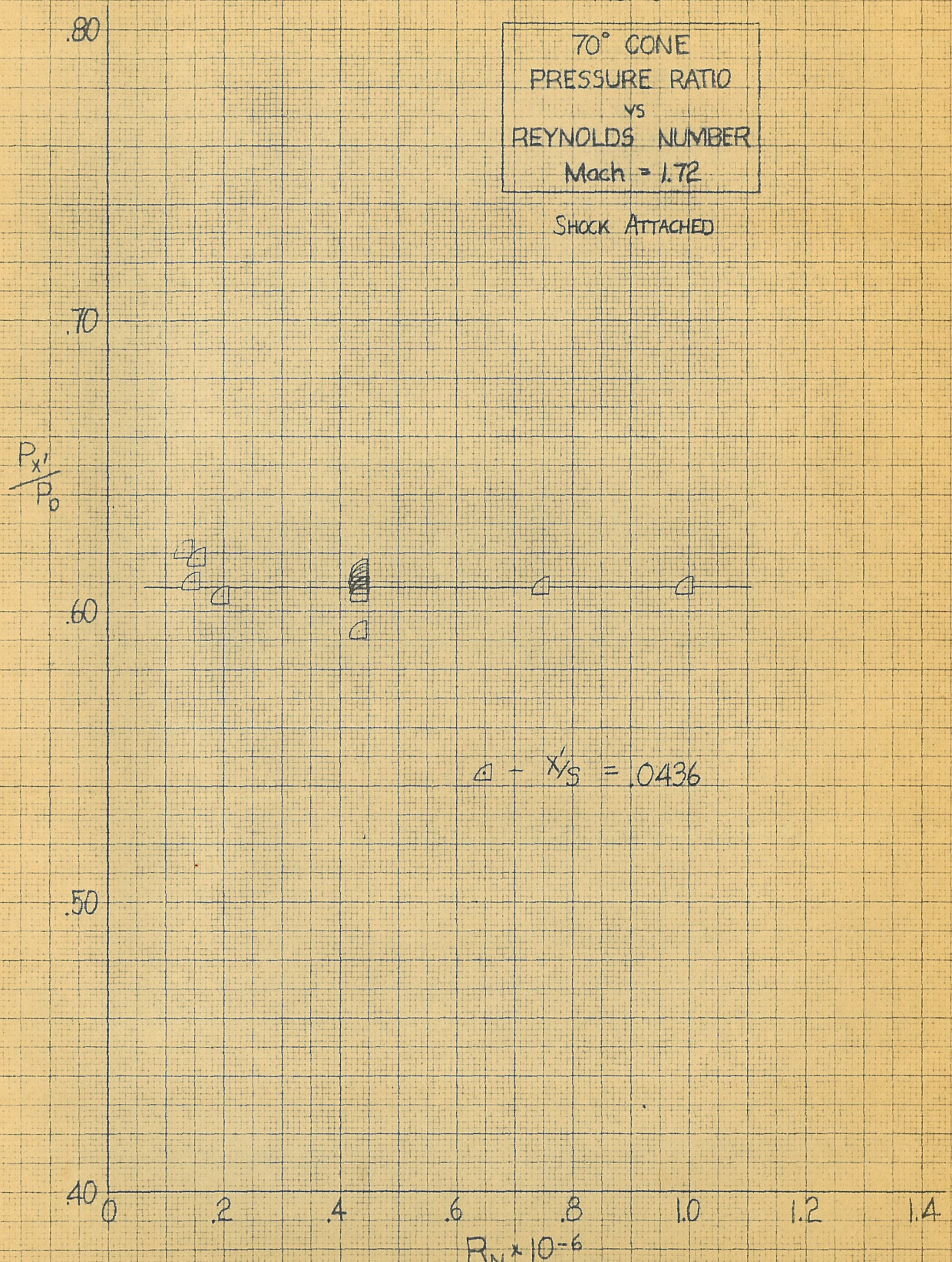
70° CONE
PRESSURE RATIO
VS
REYNOLDS NUMBER
Mach = 1.72
SHOCK ATTACHED
.80
.70
$P_{x'}/P_0$
.60
.50
.40
Δ - X'/S = .0436
0
.2
.4
.6
.8
1.0
1.2
1.4
$R_N \times 10^{-6}$

FIG. 7

70° CONE
PRESSURE RATIO
VS
REYNOLDS NUMBER
Mach = 1.72

SHOCK ATTACHED

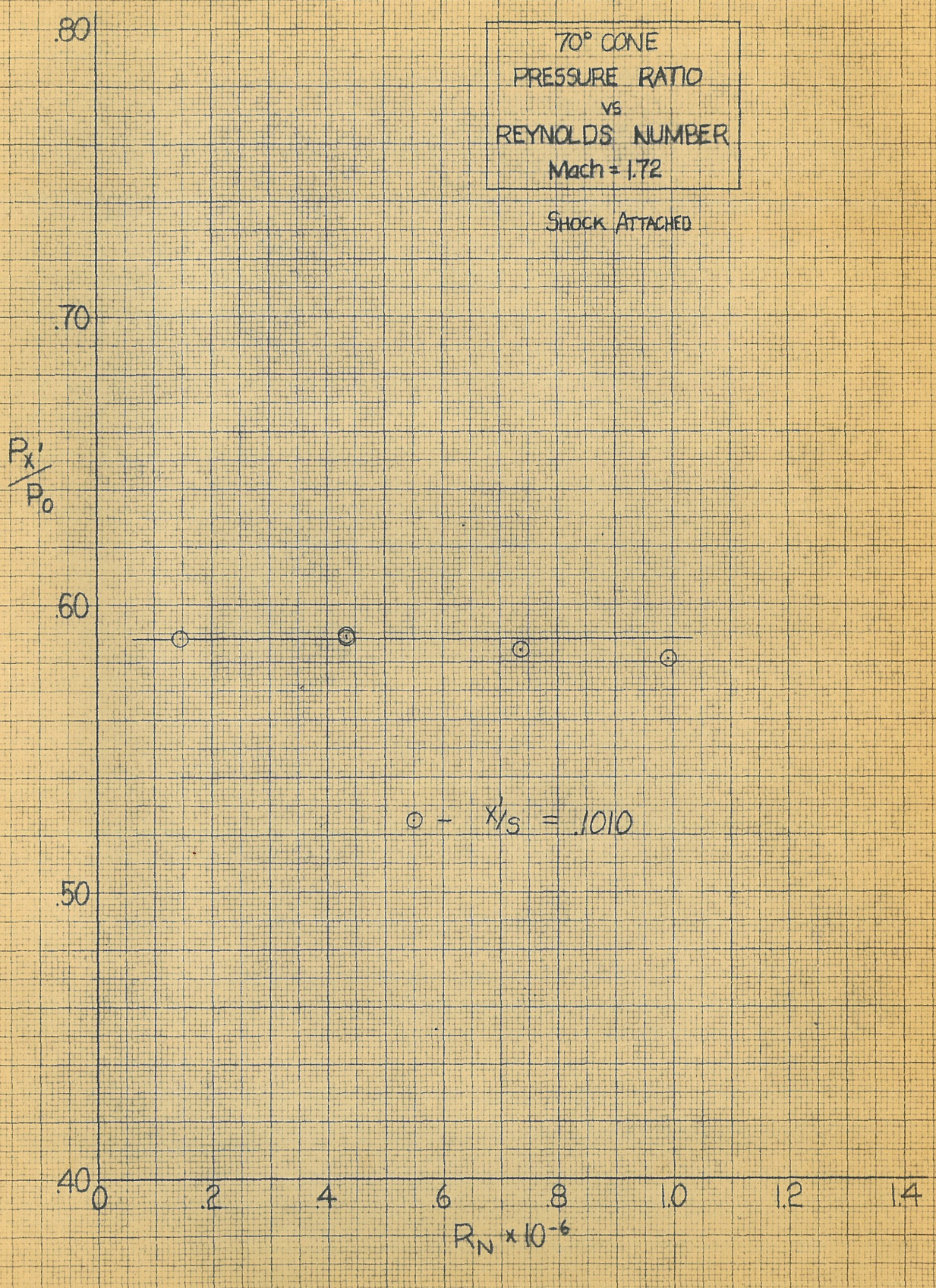

FIG. 8

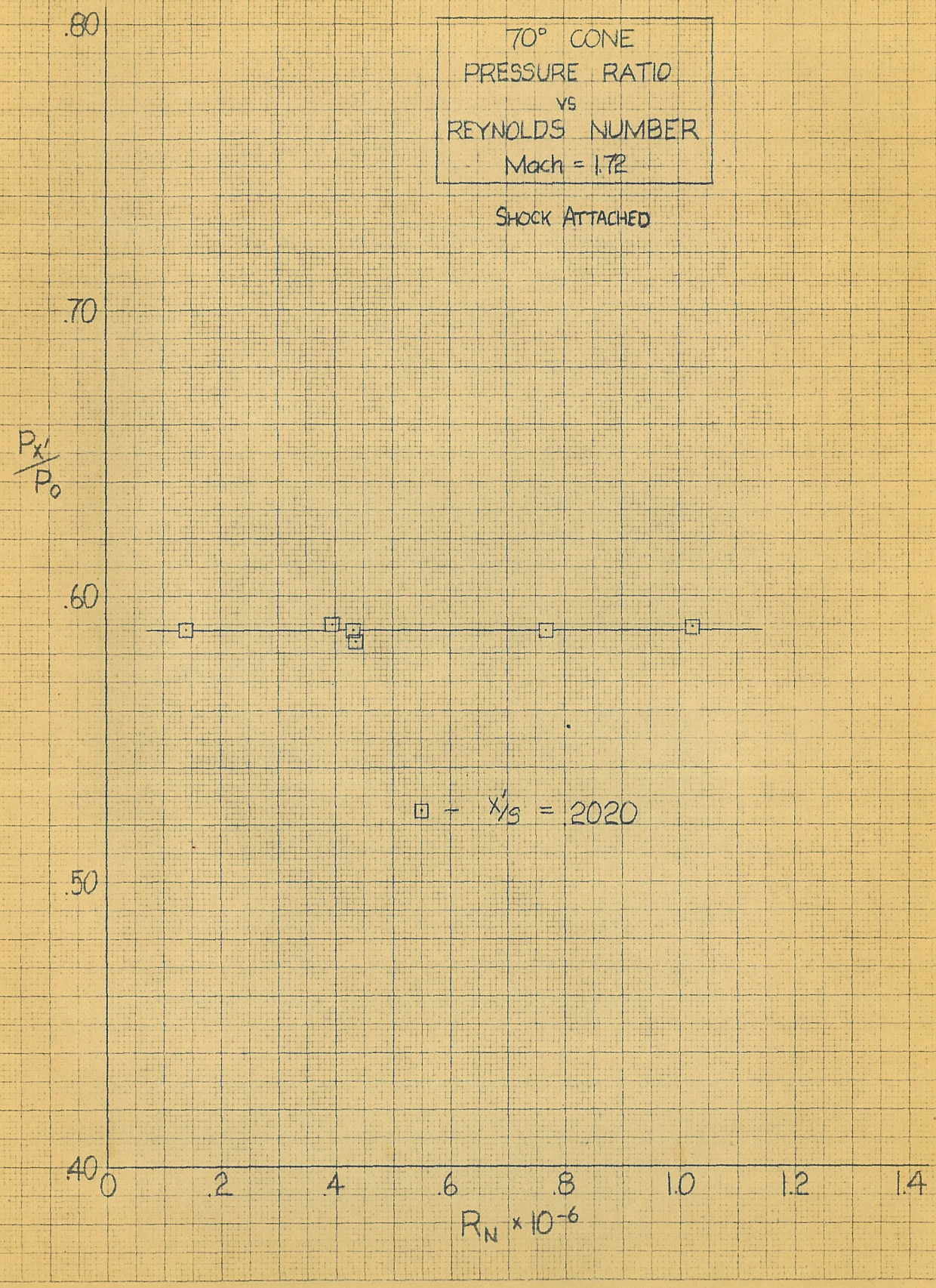
70° CONE
PRESSURE RATIO
VS
REYNOLDS NUMBER
Mach = 1.72
SHOCK ATTACHED
.80
.70
$P_{x'}/P_0$
.60
□ + X'/S = 2020
.50
.40
0
.2
.4
.6
.8
1.0
1.2
1.4
$R_N \times 10^{-6}$

FIG. 9

70° CONE
PRESSURE RATIO
VS.
REYNOLDS NUMBER
Mach = 1.72

SHOCK ATTACHED

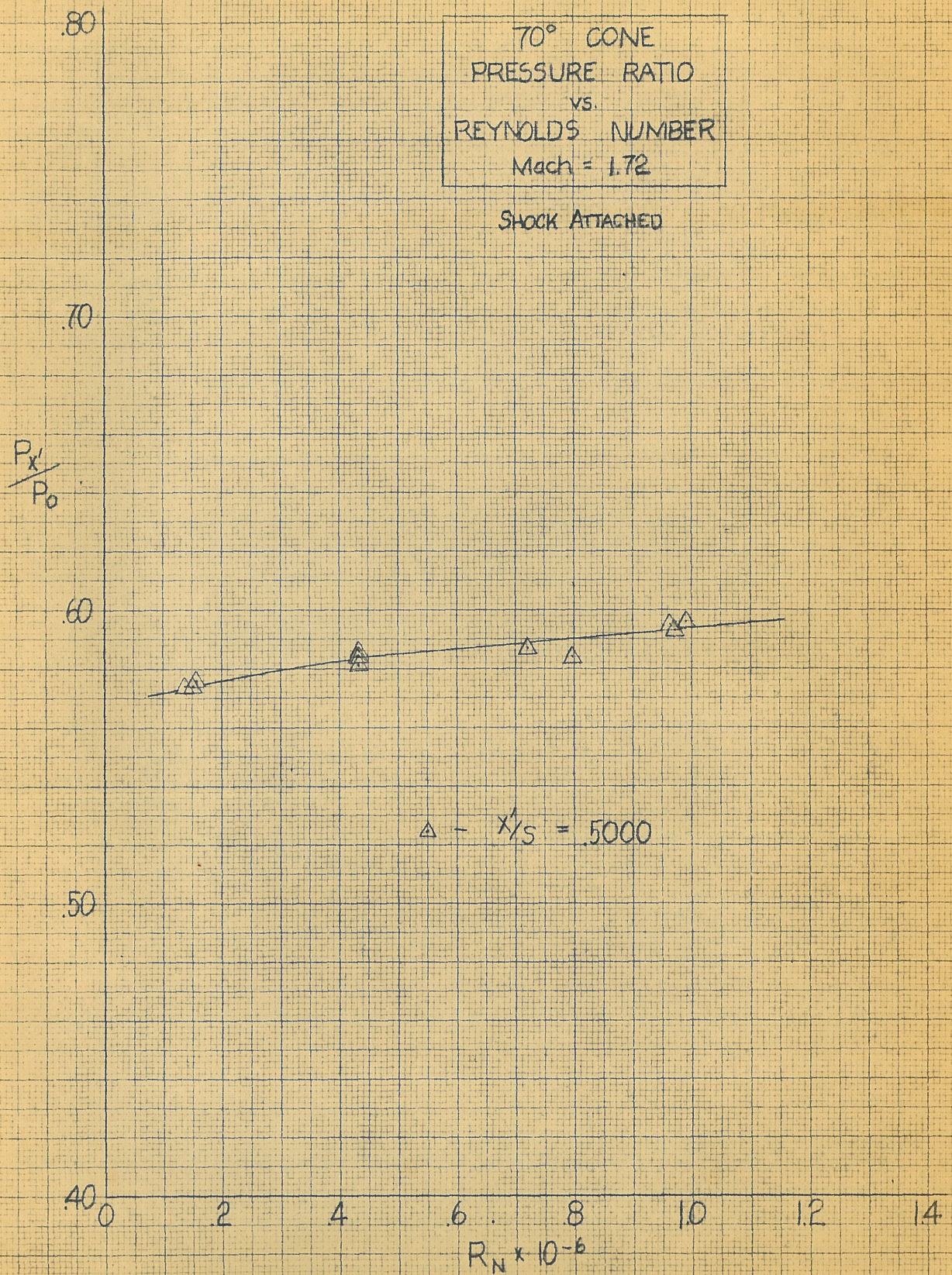

FIG. 10

70° CONE
PRESSURE DISTRIBUTION
Mach = 1.64

SHOCK DETACHED

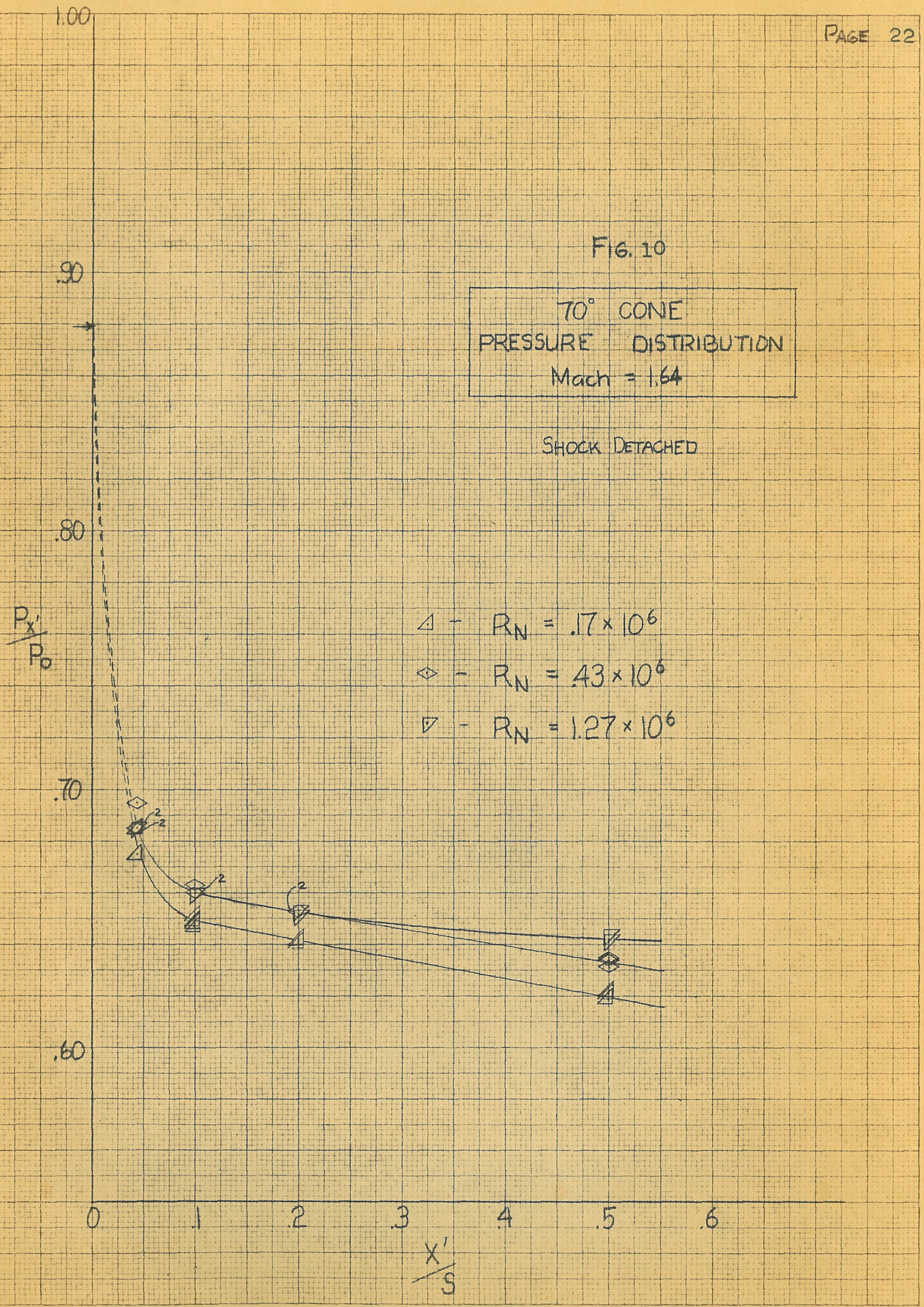

FIG. 11

70° CONE
PRESSURE DISTRIBUTION
Mach = 1.72

SHOCK ATTACHED

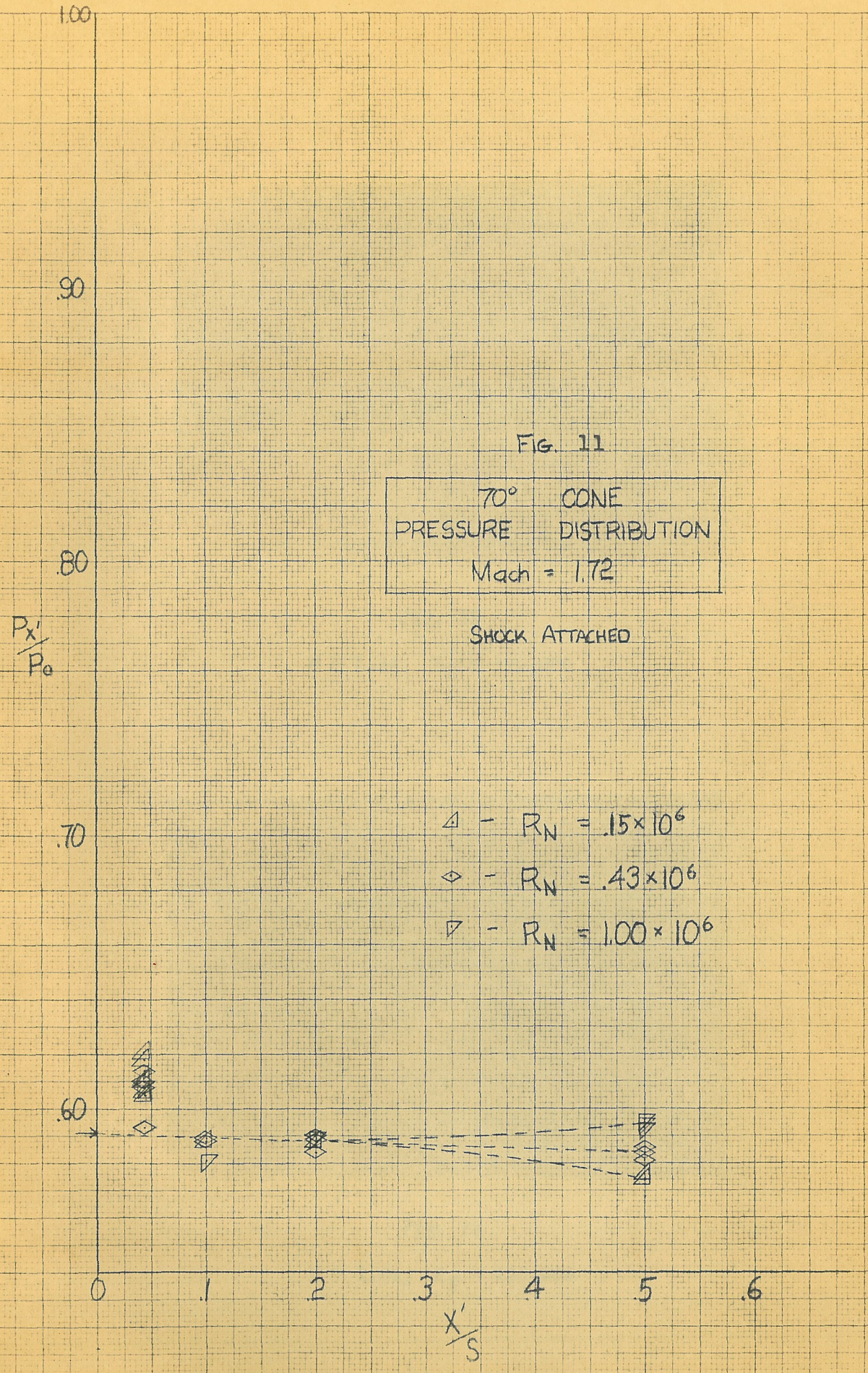

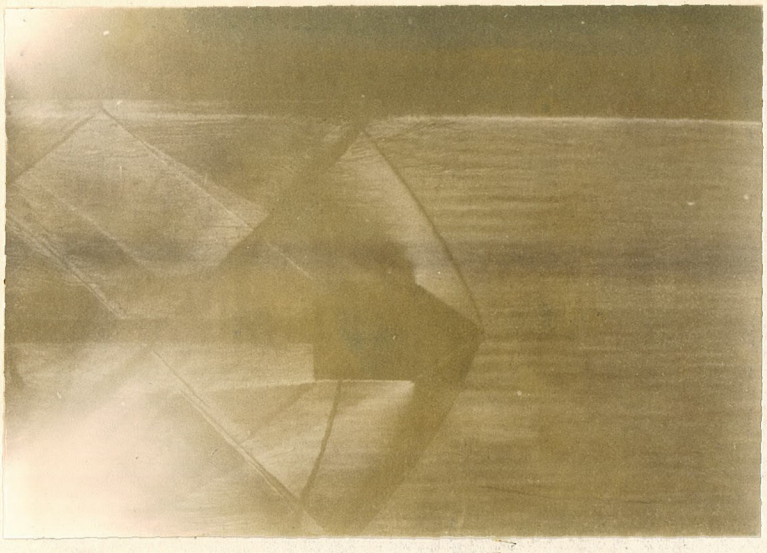

Fig. 12

$M = 1.64, \quad R_N = 170,000$

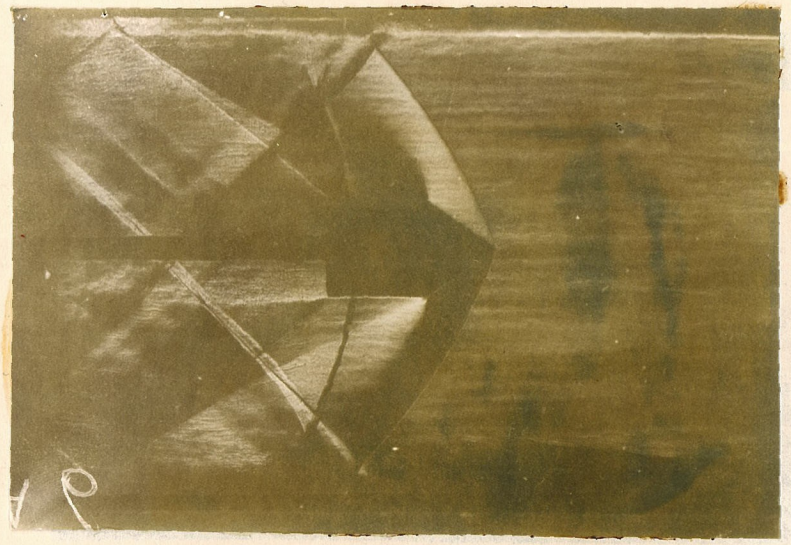

Fig. 13

$M = 1.64, \quad R_N = 430,000$

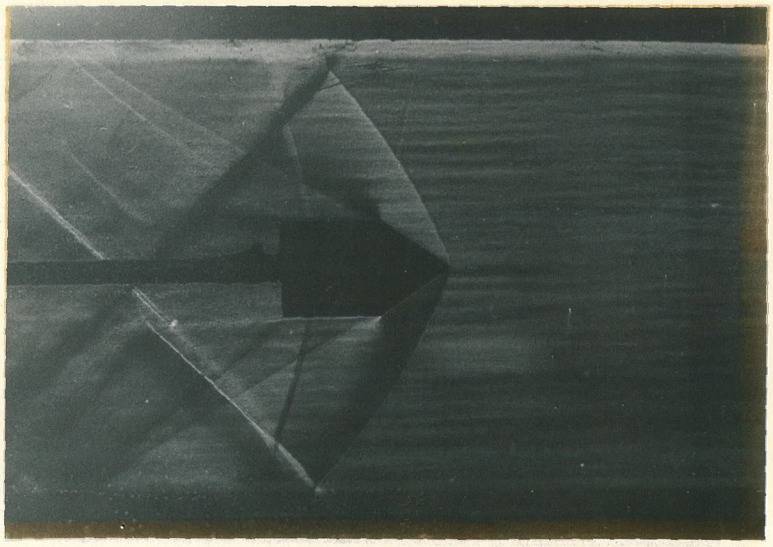

Fig. 14

$M = 1.64, \quad R_N = 1,270,000$

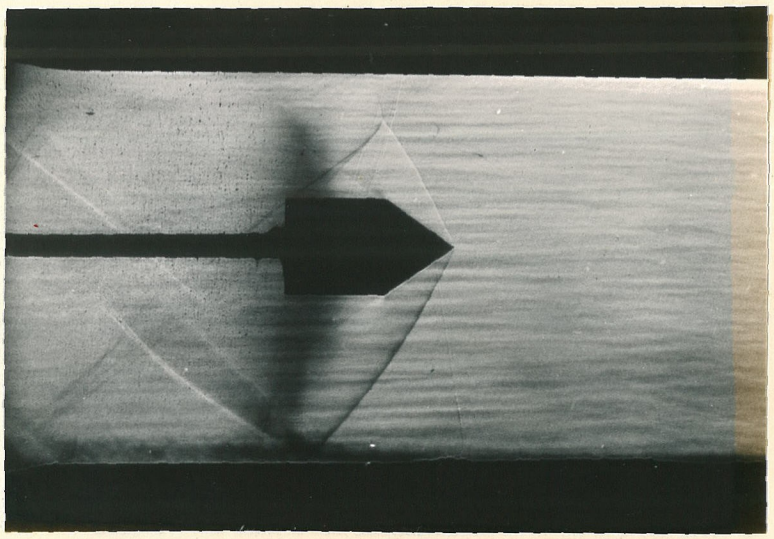

Fig. 15

$M = 1.72, \quad R_N = 150,000$

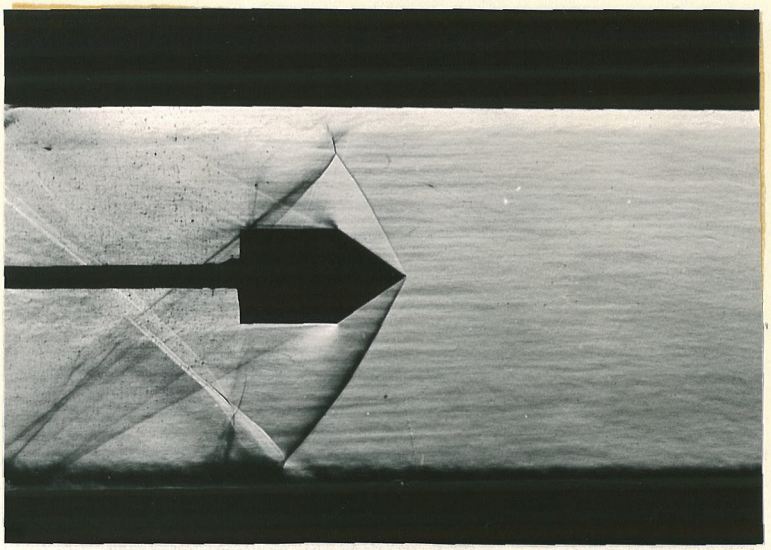

Fig. 16

$M = 1.72, \quad R_N = 430,000$

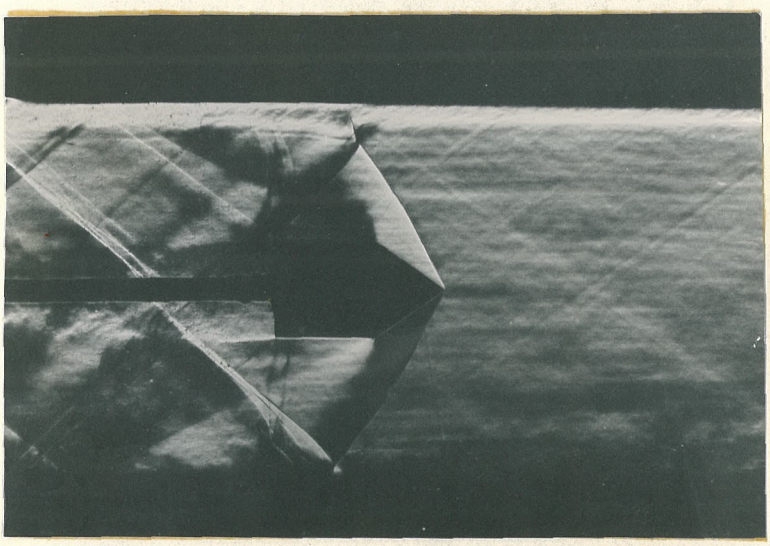

Fig. 17

$M = 1.72, \quad R_N = 1,000,000$

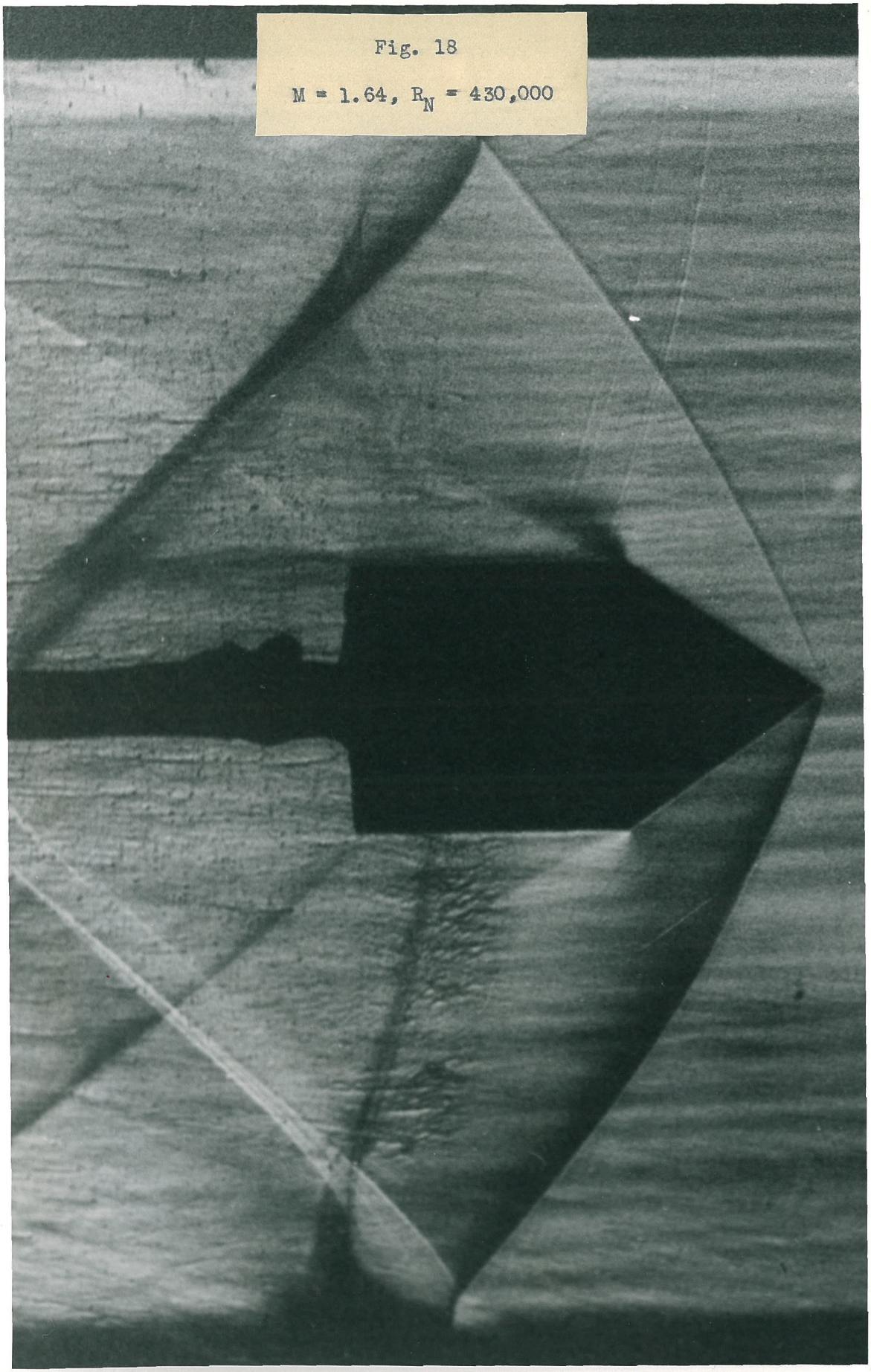

Fig. 18

$M = 1.64$, $R_N = 430{,}000$

Fig. 19

$M = 1.72$, $R_N = 430{,}000$

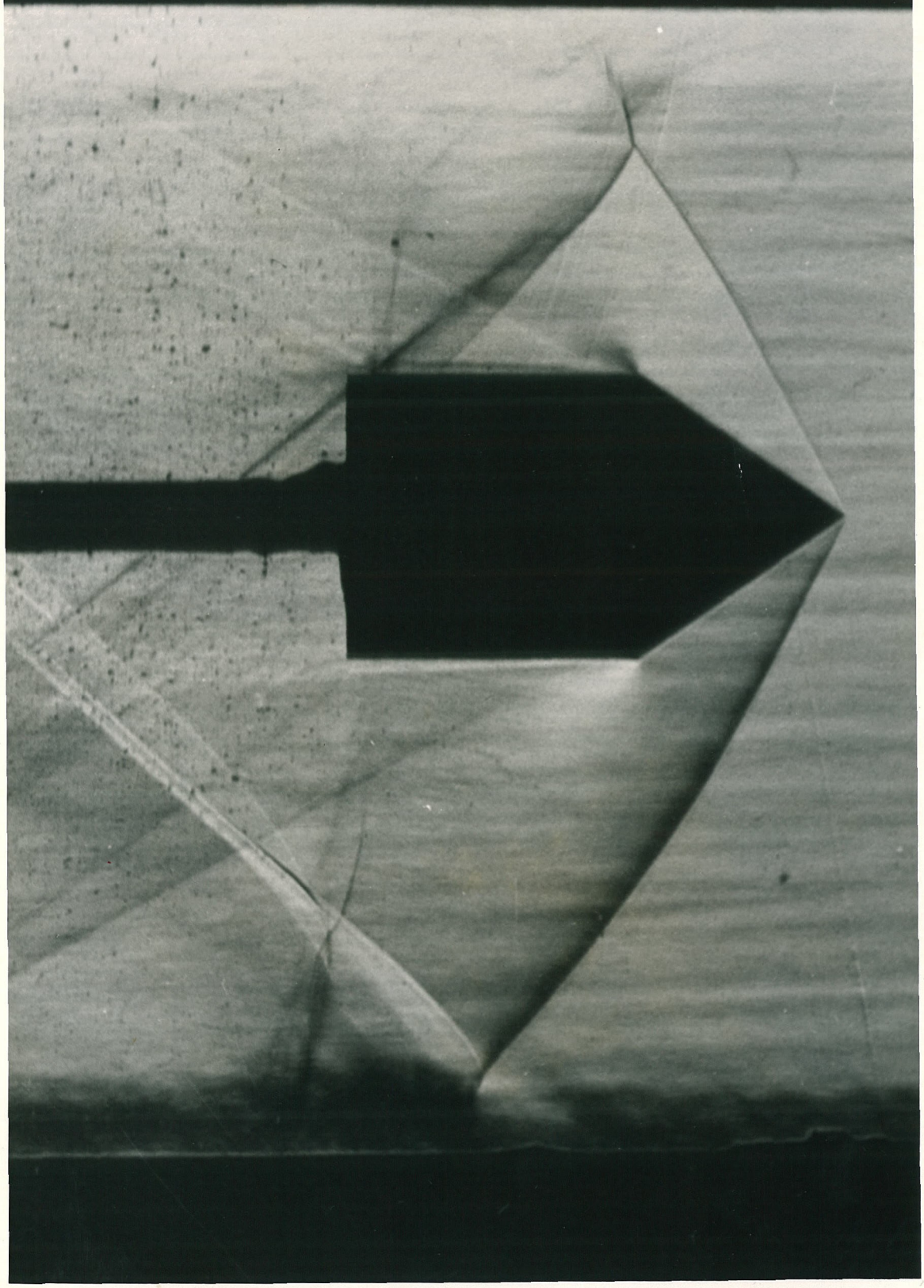

FIG. 20

70° CONE SHOCK WAVES
AT
Mach = 1.72 - ATTACHED
Mach = 1.64 - DETACHED